

Supporting Information for

Sn(II, IV) steric and electronic structure effects enable self-selective doping on Fe/Si-sites of Li₂FeSiO₄ nano-crystals for high performance lithium ion batteries

Kai Wang[†], Gaofeng Teng[†], Jinlong Yang[†], Rui Tan, Yandong Duan, Jiaxin Zheng, Feng Pan*

School of Advanced Materials, Peking University Shenzhen Graduate School, Shenzhen 518055,
People's Republic of China, E-mail: panfeng@pkusz.edu.cn

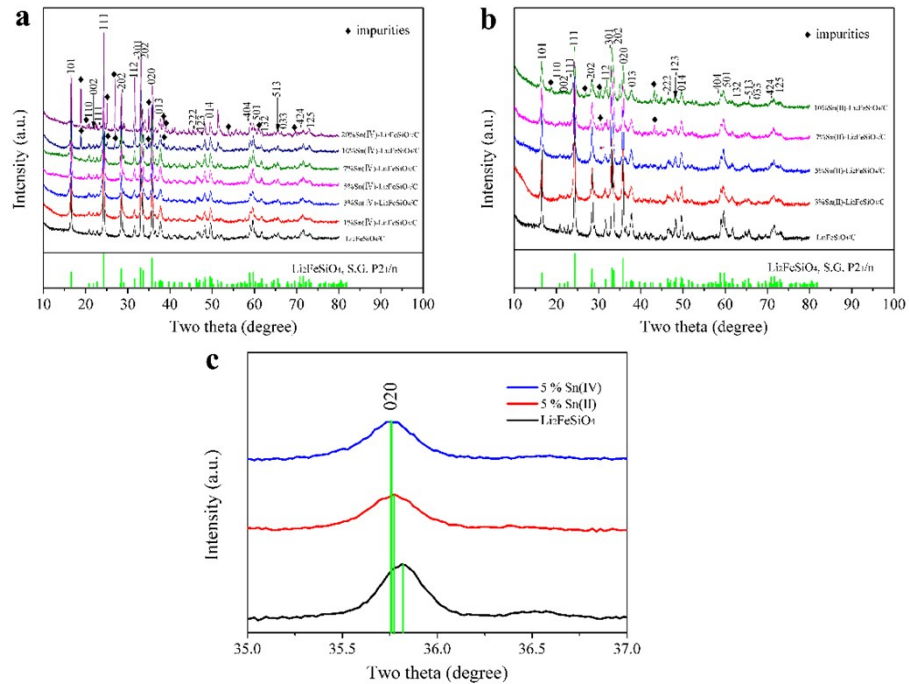


Figure S1 (a) XRD patterns of Sn(IV)-doped $\text{Li}_2\text{FeSiO}_4/\text{C}$ samples, (b) XRD patterns of Sn(II)-doped $\text{Li}_2\text{FeSiO}_4/\text{C}$ samples; (c) detailed XRD patterns of $\text{Li}_2\text{FeSiO}_4/\text{C}$, 5 % Sn(II)- $\text{Li}_2\text{FeSiO}_4/\text{C}$ and 5 % Sn(IV)- $\text{Li}_2\text{FeSiO}_4/\text{C}$ between 35° to 37°.

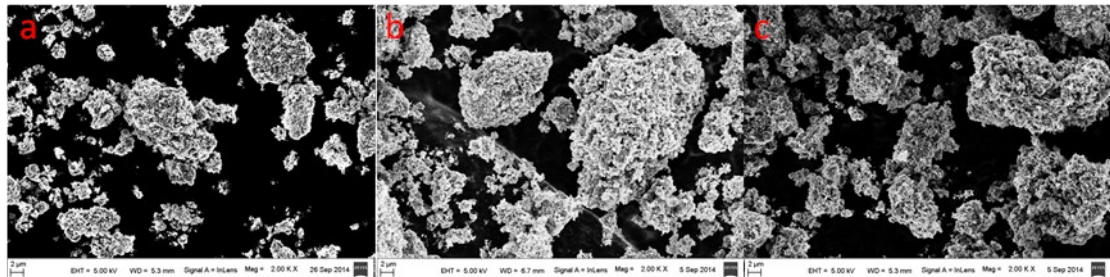


Figure S2a SEM images of (a) the pristine, (b) 5 % Sn(II) and (c) 5 % Sn(IV) doped $\text{Li}_2\text{FeSiO}_4/\text{C}$.

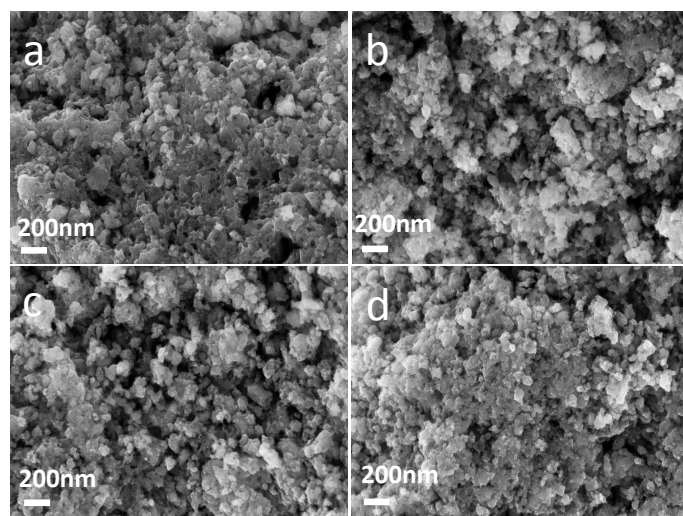


Figure S2b SEM image of different ratios of Sn(IV) doped $\text{Li}_2\text{FeSiO}_4/\text{C}$ samples: (a) 1 %, (b) 3 %, (c) 5 %, (d) 7 %.

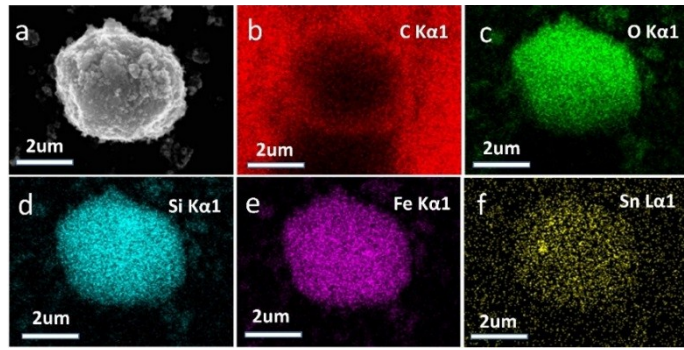


Figure S3a EDS mapping of 5 % Sn(II)-Li₂FeSiO₄/C.

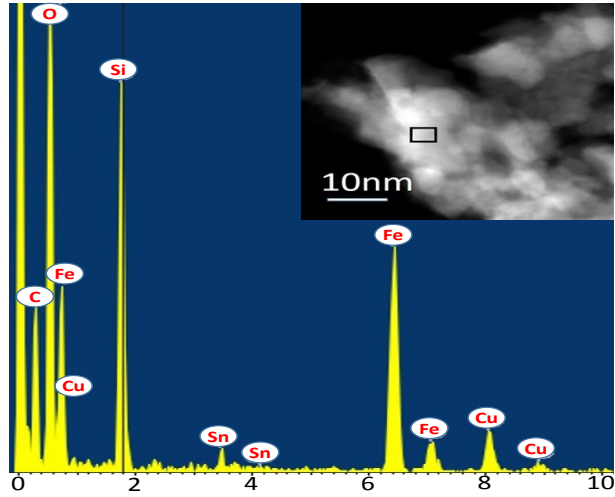


Figure S3b EDS mapping of 5 % Sn(II)-Li₂FeSiO₄/C obtained by TEM test in a small scale bar (the rectangular block in the insert picture is the EDS mapping zone).

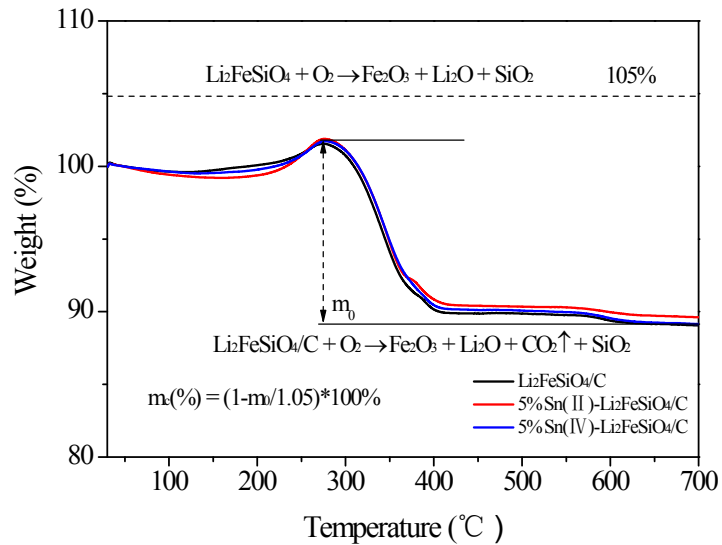


Figure S4 TG analysis of Li₂FeSiO₄/C, 5 % Sn(II)-Li₂FeSiO₄/C and 5 % Sn(IV)-Li₂FeSiO₄/C.

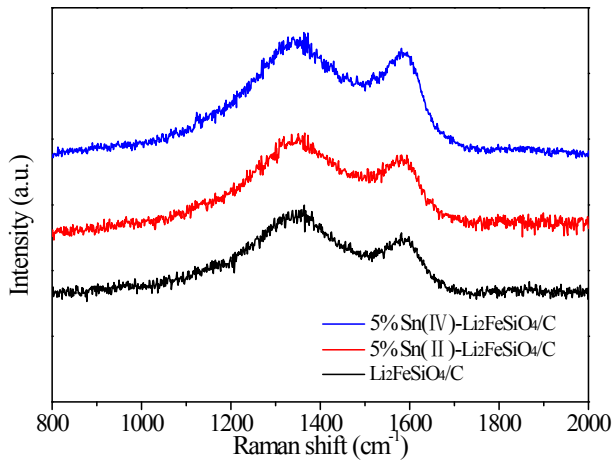


Figure S5 Raman spectra of $\text{Li}_2\text{FeSiO}_4/\text{C}$, 5 % Sn(II)- $\text{Li}_2\text{FeSiO}_4/\text{C}$ and 5 % Sn(IV)- $\text{Li}_2\text{FeSiO}_4/\text{C}$.

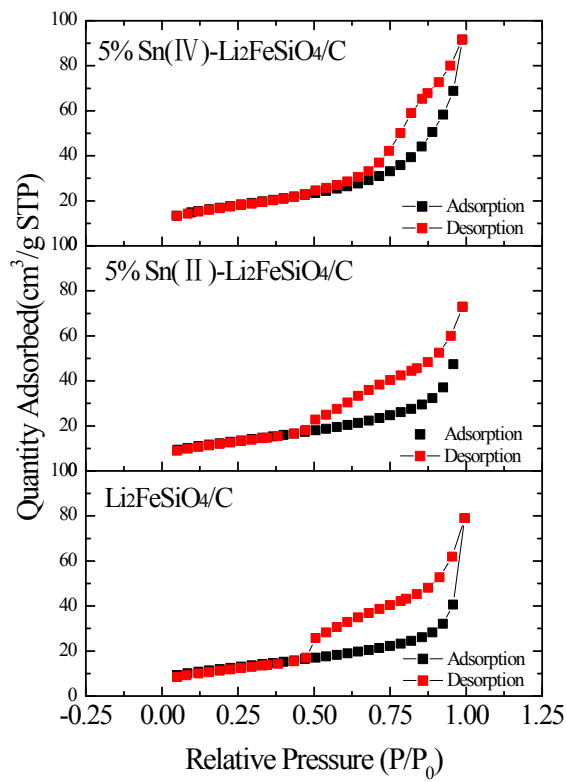


Figure S6 Nitrogen adsorption and desorption isotherms at 77.47 K.

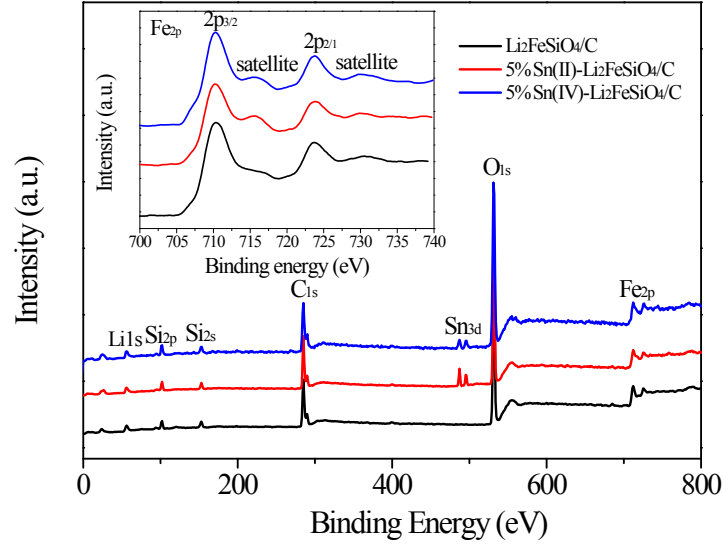


Figure S7 XPS spectra of samples (the insert picture is the spectra of Fe2p). Fe 2p spectra of all of the three samples are split in two parts due to spin-orbit coupling, namely Fe 2p_{3/2} and Fe 2p_{1/2}, with an intensity ratio of about 2/1. Each part consists of a main peak and a “shake-up” satellite.¹ For Li₂FeSiO₄, Fe 2p_{3/2} main peak at 710 eV with a satellite peak at 715 eV, and Fe 2p_{1/2} main peak at 724 eV with a satellite peak at 729 eV, meaning that tin doping doesn't affect the valance state of iron in Li₂FeSiO₄, the oxidation state of Fe in all of the three samples is +2.

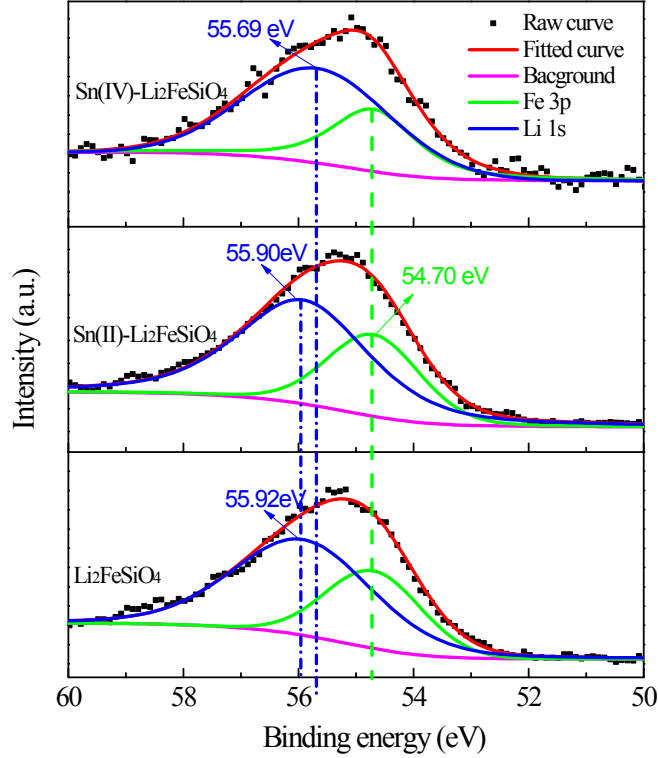


Figure S8. Fitted Li 1s and Fe 3p spectra of spectra of Li₂FeSiO₄/C, 5 % Sn(II)-Li₂FeSiO₄/C and 5 % Sn(IV)-Li₂FeSiO₄/C.

Table S1 Ratios of Sn(II) and Sn(IV) in different amount of Sn(IV) doped $\text{Li}_2\text{FeSiO}_4/\text{C}$ samples.

Samples	Sn(II)	Sn(IV)
1 % doping	64.4 %	35.6 %
3 % doping	61.0 %	39.0 %
5 % doping	41.6 %	58.4 %
7 % doping	33.7 %	66.3 %

Table S2.1 Atomic coordination for the pristine $\text{Li}_2\text{FeSiO}_4$ obtained from Rietveld refinement.

Site	Np	x	y	z	Atom	Occ
Li1	4	0.66300	0.78500	0.66900	Li+	1
Li2	4	0.58500	0.19300	0.08400	Li+	1
Fe1	4	0.28934(62)	0.79877(59)	0.54376(59)	Fe2+	1
Si1	4	0.04110(97)	0.8040(12)	0.7971(10)	Si4+	1
O1	4	0.8646(23)	0.7031(25)	0.8167(21)	O2-	1
O2	4	0.4221(23)	0.2168(17)	0.8933(22)	O2-	1
O3	4	0.6914(23)	0.7685(20)	0.4322(22)	O2-	1
O4	4	0.9665(15)	0.8618(14)	0.2078(15)	O2-	1

Table S2.2 Atomic coordination for the 5 % Sn(II)- $\text{Li}_2\text{FeSiO}_4$ obtained from Rietveld refinement.

Site	Np	x	y	z	Atom	Occ
Li1	4	0.66300	0.78500	0.66900	Li+	1
Li2	4	0.58500	0.19300	0.08400	Li+	1
Fe1	4	0.28013(58)	0.79368(84)	0.55101(50)	Fe2+	0.95
					Sn2+	0.05
Si1	4	0.0353(12)	0.8138(15)	0.8020(12)	Si4+	1
O1	4	0.8848(24)	0.7359(39)	0.8139(23)	O2-	1
O2	4	0.4187(24)	0.2219(22)	0.9073(23)	O2-	1
O3	4	0.6993(22)	0.7788(29)	0.4389(19)	O2-	1
O4	4	0.9828(19)	0.8490(21)	0.1986(18)	O2-	1

Table S2.3 Atomic coordination for the 5 % Sn(IV)- $\text{Li}_2\text{FeSiO}_4$ obtained from Rietveld refinement.

Site	Np	x	y	z	Atom	Occ
Li1	4	0.66300	0.78500	0.66900	Li+	1
Li2	4	0.58500	0.19300	0.08400	Li+	1
Fe1	4	0.29560(61)	0.79769(73)	0.53460(61)	Fe2+	0.9792
					Sn2+	0.0208
Si1	4	0.04829(86)	0.8130(13)	0.78591(93)	Si4+	0.9708
					Sn4+	0.0292
O1	4	0.8433(22)	0.7125(40)	0.8246(25)	O2-	1
O2	4	0.4301(23)	0.2121(20)	0.8842(23)	O2-	1
O3	4	0.6850(22)	0.7826(22)	0.4390(23)	O2-	1
O4	4	0.9575(16)	0.8518(16)	0.2129(18)	O2-	1

Table S3 the calculated effective radius of Fe²⁺, Si⁴⁺, Sn⁴⁺, Sn²⁺ in tetrahedra.

	r ₀ (Å)	k	z	r _{k-calculated} (Å)	r _{k-reference2} (Å)
Fe ²⁺	0.286	4	+2	0.59	0.63
Si ⁴⁺	-0.076	4	+4	0.26	0.26
Sn ⁴⁺	0.318	4	+4	0.57	0.55
Sn ²⁺	0.781	4	+2	1.00	none

the effective radius of Fe²⁺, Si⁴⁺, Sn⁴⁺, Sn²⁺ in tetrahedra (r_{k-calculated} (Å)) were calculated by the relationship between the cationic radii and the coordination number:³

$$r_k = r_0 + dk - \frac{0.0236k}{z}$$

where r₀ is the radius of free cation, z is the valence, k is the coordination number and

$$d = 0.1177 - 0.0081z - 0.0347r_0 - 0.0050zr_0$$

Table S4. Calculated Lattice Parameters (in Å) and Volume (in Å³) for Li_xFeSiO₄, Li_xFe_{0.94}Sn_{0.06}SiO₄ and Li_xFeSi_{0.94}Sn_{0.06}O₄ (x = 0, 0.5, 1, 2)

	a / Å	b / Å	c / Å	V/Å ³ (f.u) ⁻¹	ΔV/V
Li ₂ FeSiO ₄	10.045	10.985	12.534	86.46	
LiFeSiO ₄	10.163	10.458	13.402	89.04	2.98 %
Li _{0.5} FeSiO ₄	10.349	10.567	13.685	93.52	8.17 %
FeSiO ₄	10.756	10.835	14.969	109.03	26.1 %
Li ₂ Fe _{0.94} Sn _{0.06} SiO ₄	10.083	11.020	12.549	87.16	
LiFe _{0.94} Sn _{0.06} SiO ₄	10.161	10.446	13.502	89.58	2.77 %
Li _{0.5} Fe _{0.94} Sn _{0.06} SiO ₄	10.365	10.626	13.614	93.72	7.52 %
Fe _{0.94} Sn _{0.06} SiO ₄	10.734	10.843	14.981	108.97	25.02 %
Li ₂ FeSi _{0.94} Sn _{0.06} O ₄	10.063	11.026	12.581	87.25	
LiFeSi _{0.94} Sn _{0.06} O ₄	10.196	10.492	13.463	90.03	3.19 %
Li _{0.5} FeSi _{0.94} Sn _{0.06} O ₄	10.406	10.580	13.742	94.58	8.40 %
FeSi _{0.94} Sn _{0.06} O ₄	10.776	10.792	15.012	109.12	25.07 %

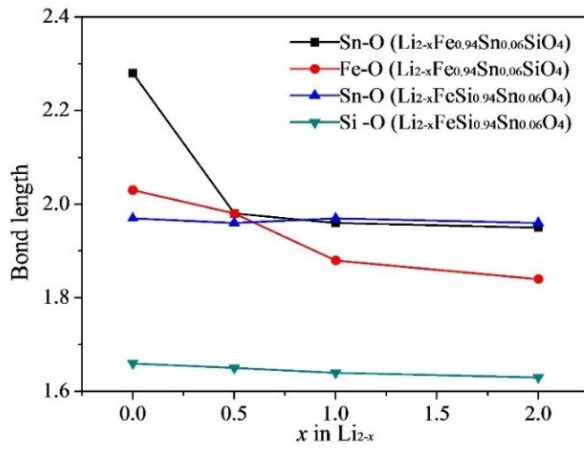


Figure S9. The calculated average bond length for SnO_4 and FeO_4 in $\text{Li}_x\text{Fe}_{0.94}\text{Sn}_{0.06}\text{SiO}_4$, SnO_4 and SiO_4 in $\text{Li}_x\text{FeSi}_{0.94}\text{Sn}_{0.06}\text{O}_4$.

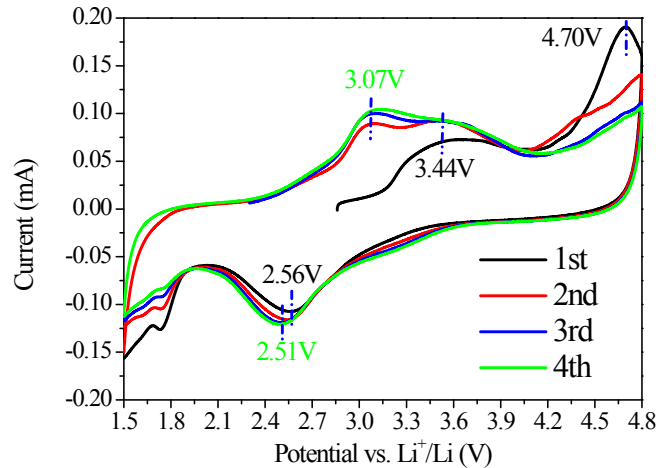


Figure S10. Cyclic voltammograms of 5 % Sn(II)- $\text{Li}_2\text{FeSiO}_4/\text{C}$ at 0.2 mV s^{-1} .

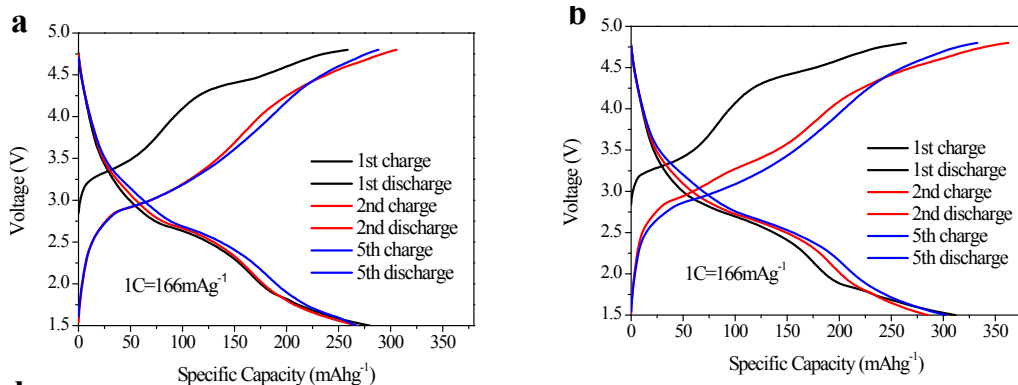


Figure S11. Charge-discharge profiles of (a) $\text{Li}_2\text{FeSiO}_4/\text{C}$ and (b) 5 % Sn(II)- $\text{Li}_2\text{FeSiO}_4/\text{C}$ at 0.2 C ($1\text{C} = 166 \text{ mA g}^{-1}$).

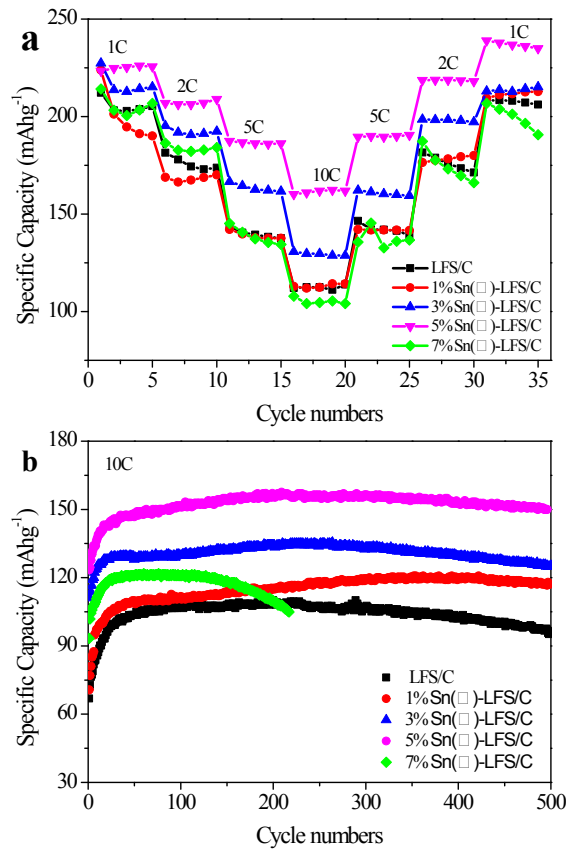


Figure S12. (a) Cyclic performance of different ratios of Sn(IV) doped $\text{Li}_2\text{FeSiO}_4$ at different rates, (b) Long-term high rate cycling life of different ratios of Sn(IV) doped $\text{Li}_2\text{FeSiO}_4$ at 10 C for 500 cycles.

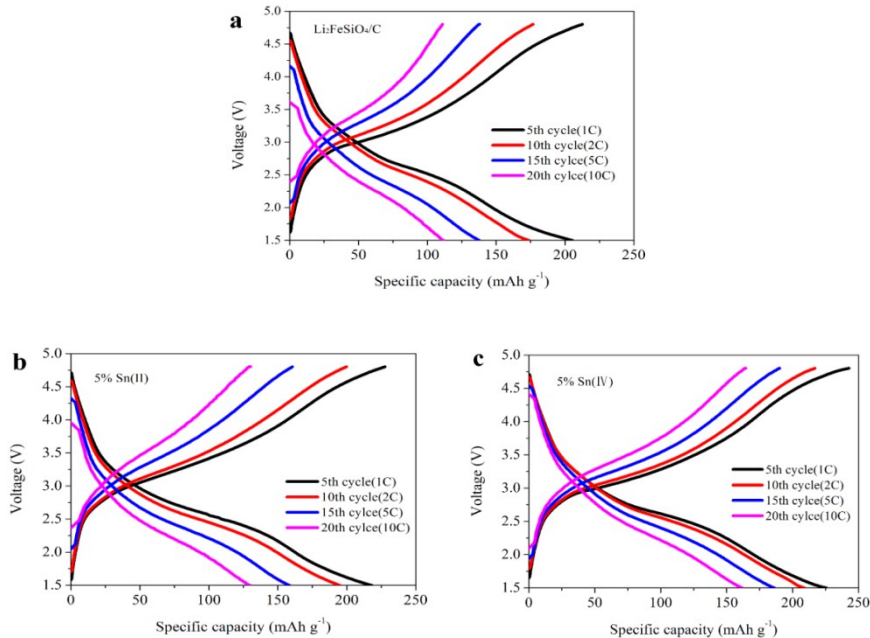


Figure S13 Typic charge-discharge curves of these three samples at various rates.

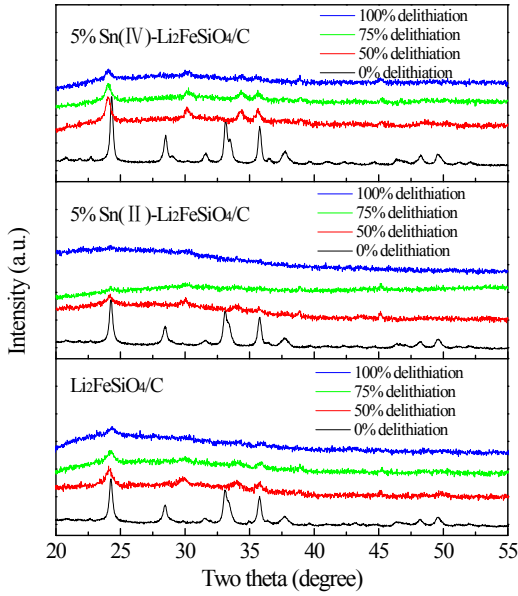
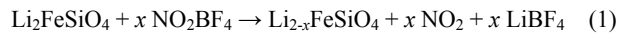


Figure S14. XRD patterns after chemical extraction of lithium. Bottom: material Li₂FeSiO₄/C, middle: material 5 % Sn(II)-Li₂FeSiO₄/C, top: 5 % Sn(IV)-Li₂FeSiO₄/C.

Chemical extraction of lithium from the samples were carried out by using the oxidizer, NO₂BF₄ (95+ % purity, Aldrich), in acetonitrile medium at room temperature with constantly stirring for 48 hours. The reaction process is the following:



The high reactivity of NO₂BF₄ lead to the possibilities of its decomposition and side reactions, the experiments invariably required more amounts of the oxidizer.⁴ Here, the NO₂BF₄ were added 25 % more than the theoretical value. The Li-ions were extracted by the following percentage: 50 %, 75 % and 100 %, equaling to 1 Li, 1.5 Li and 2 Li extraction from all the three samples, respectively.

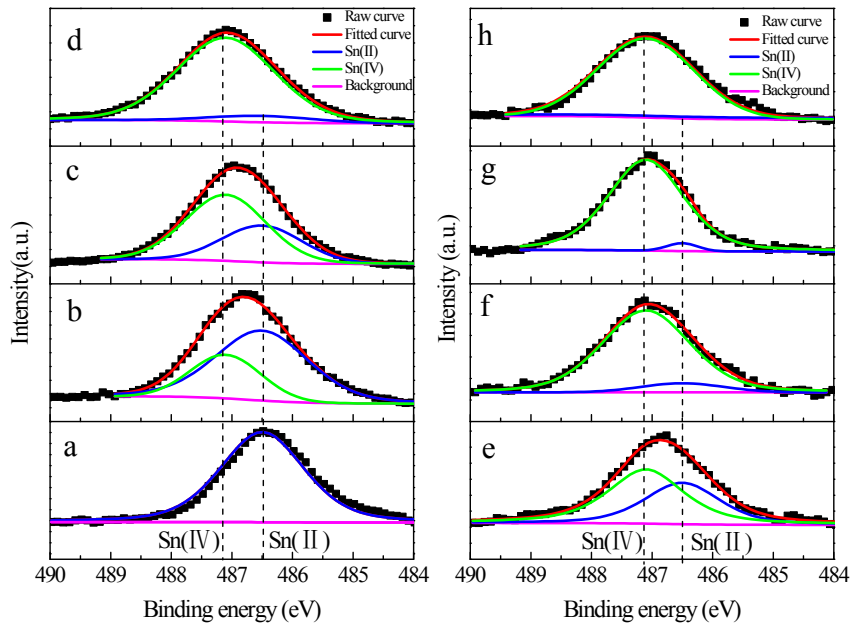


Figure S15. (1) Sn 3d 5/2 spectra of 5 % Sn(II)-Li₂FeSiO₄/C, with chemical delithiation: (a) 0 %, (b) 50 %, (c) 75 %, (d) 100 %;

(2) Sn 3d 5/2 spectra of 5 % Sn(IV)-Li₂FeSiO₄/C with chemical delithiation: (a) 0 %, (b) 50 %, (c) 75 %, (d) 100 %.

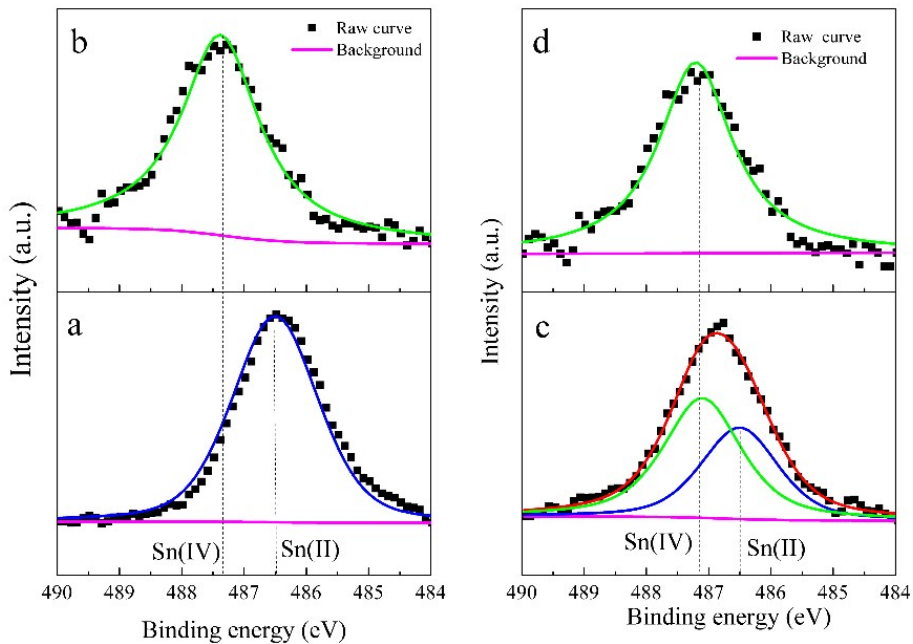


Figure S16. Sn 3d 5/2 spectra of (1) 5 % Sn(II)- $\text{Li}_2\text{FeSiO}_4/\text{C}$ electrode (a) before charged (b) after fully charged at 4.8 V; (2) 5 % Sn(IV)- $\text{Li}_2\text{FeSiO}_4/\text{C}$ electrode (c) before charged (d) after fully charged at 4.8 V.

Table S5. Sn(II) and Sn(IV) content fitted by Sn3d 5/2 of 5 % Sn(II)- $\text{Li}_2\text{FeSiO}_4$ and 5 % Sn(IV)- $\text{Li}_2\text{FeSiO}_4$ after chemical extraction of lithium.

	Sn(II)	Sn(IV)
5 % Sn(II)- $\text{Li}_2\text{FeSiO}_4$		
0 % delithiated	100 %	0
50 % delithiated	70.1 %	29.9 %
75 % delithiated	35.1 %	64.9 %
100 % delithiated	6.9 %	93.1 %
5 % Sn(IV)- $\text{Li}_2\text{FeSiO}_4$		
0 % delithiated	41.6 %	58.4 %
50 % delithiated	8.4 %	91.6 %
75 % delithiated	2.9 %	97.1 %
100 % delithiated	0	100 %

References

1. R. Dedryvere, M. Maccario, L. Croguennec, F. Le Cras, C. Delmas and D. Gonbeau, *Chem Mater*, 2008, **20**, 7164-7170.
2. R. t. Shannon, *Acta Crystallographica Section A: Crystal Physics, Diffraction, Theoretical and General Crystallography*, 1976, **32**, 751-767.
3. J. Zio, *J Solid State Chem*, 1985, **57**, 269-290.
4. S. Venkatraman and A. Manthiram, *Chem Mater*, 2002, **14**, 3907-3912.